Supporting Information

Optoelectronic Properties of a van der Waals WS_2 Monolayer/2D Perovskite Vertical Heterostructure

Qixing Wang[†,‡,¶], Qi Zhang[†,¶], Xin Luo[§,¶], Junyong Wang[†], Rui Zhu[†], Qijie Liang[†,∥], Lei Zhang[†], Justin Zhou Yong[†], Calvin Pei Yu Wong[⊥], Goki Eda[†,#,∇], Jurgen H. Smet[‡], and Andrew T. S. Wee[†,#]*

[†]Department of Physics, National University of Singapore, 2 Science Drive 3, Singapore 117542, Singapore

[‡]Max Planck Institute for Solid State Research, Stuttgart D-70569, Germany (current position)

[§]State Key Laboratory of Optoelectronic Materials and Technologies, Centre for Physical Mechanics and Biophysics, School of Physics, Sun Yat-sen University, Guangzhou 510275, P.R. China

[∥]SZU-NUS Collaborative Innovation Center for Optoelectronic Science & Technology, Key Laboratory of Optoelectronic Devices and Systems of Ministry of Education and Guangdong Province, College of Optoelectronic Engineering, Shenzhen University, Shenzhen 518060, China

[⊥]Institute of Materials Research and Engineering (IMRE), Agency for Science, Technology and Research (A*STAR), 2 Fusionopolis Way, Innovis #08-03, Singapore 138634, Singapore

#Centre for Advanced 2D Materials, National University of Singapore, Block S14, 6 Science Drive 2, Singapore 117546, Singapore

∇Department of Chemistry, National University of Singapore, 3 Science Drive 3, 117543, Singapore

¶These authors contributed equally to this work

Corresponding author: Andrew T. S. Wee (Email: phyweets@nus.edu.sg, Tel: +65 66013757)

1. AFM image for the determination of the PEPI thickness

In Figure S1, we show an optical image of the monolayer WS_2/PEPI van der Waals heterostructure used for optical measurements together with an AFM profile of a portion of this image where only the PEPI layer is present in order to estimate the height of this layer.

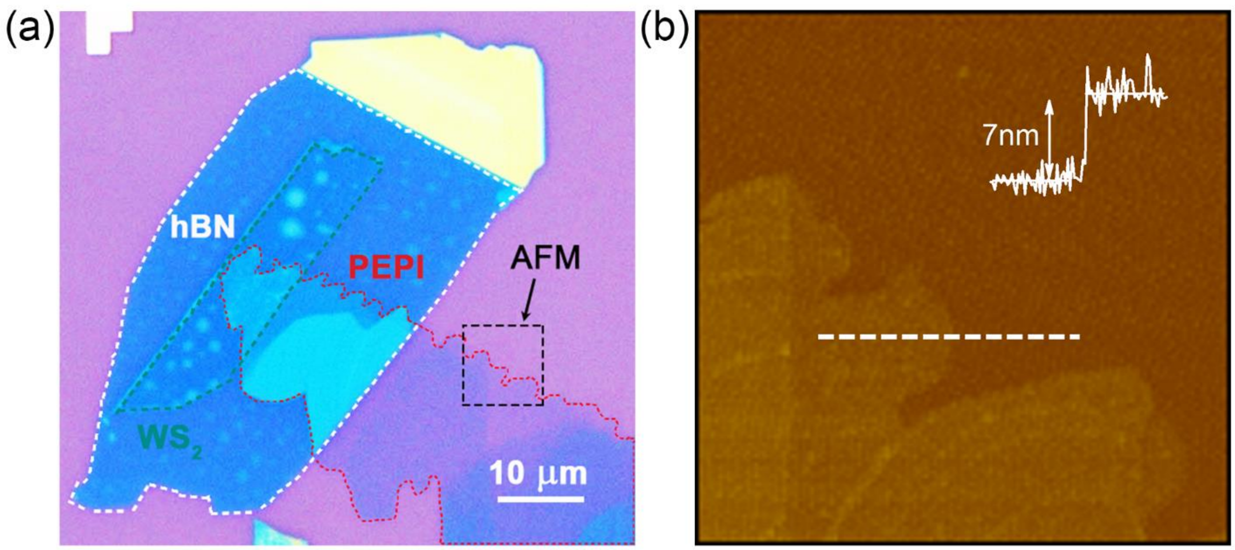

Figure S1. (a) Optical microscope image of the monolayer WS_2/PEPI heterostructure. The black dashed square demarcates the region where an AFM measurement was performed in order to determine the thickness of the PEPI layer. The optical contrast in this region is similar to the region bordered by the red dashed lines in **Figure 1**b of the main text. (b) AFM image of the area marked in panel (a). The scanning area is 10 µm × 10 µm. A line scan along the white dashed line is shown as an inset and yields an estimate for the PEPI thickness of about 7nm.

2. Performance of a parallel device geometry

Figure S2 shows the device structure and the corresponding optoelectronic device performances of a WS_2/PEPI heterostructure device without separate contacts to each layer. Instead, both layers are contacted in parallel by the source and the drain contact on either side of the device. For this device architecture, the enhancement of the photoresponsivity in the WS_2/PEPI region compared to that in the WS_2 monolayer region is very small. This parallel connection does not allow for efficient extraction/separation of the photo-generated charge carriers through a built-in or applied electric field at the heterointerface.

In contrast, in the device geometry of Figure 2a, it is possible to generate an additional built-in potential at the heterointerface by applying a bias voltage. This causes a significant improvement in the efficiency for charge separation and extraction. As a result, the photoresponsivity in the WS_2/PEPI heterointerface region is enhanced by nearly a factor of 5 compared to that in the WS_2 monolayer region.

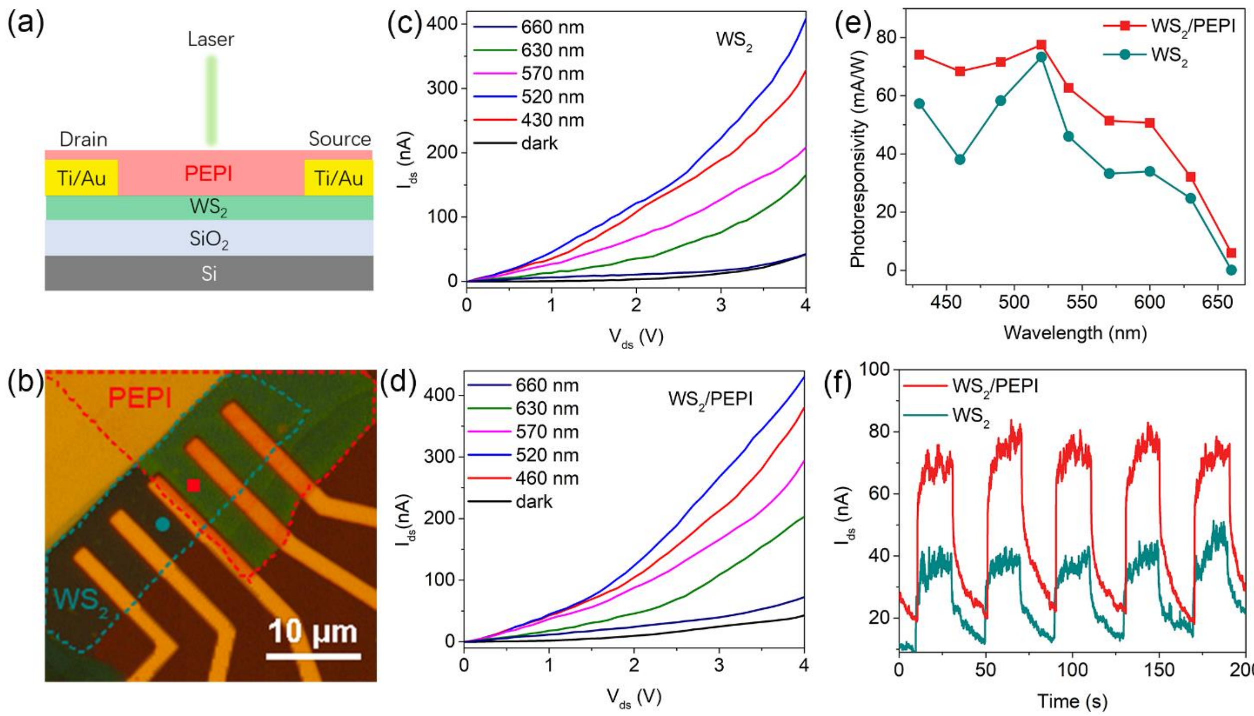

Figure S2. Performance of the WS_2/PEPI heterostructure photodetector with both layers contacted in parallel. (a) Schematic device structure of this parallel device structure. (b) Optical microscope image. The red square and the cyan circle mark the approximate location of the laser spot during the optoelectronic measurements. (c,d). I_{ds}-V_{ds} curves recorded on the WS_2 monolayer region (c) and the WS_2/PEPI interface region (d) in the dark and for laser illuminations with different wavelengths. The laser power for illumination is 5 µW in each case. The gate voltage V_g is set to 0 V. (e) A comparison of the photoresponsivity measured on the WS_2 monolayer region and the WS_2/PEPI heterointerface region for V_g = 0 V and V_{ds} = 4 V. (f) A comparison of I_{ds} versus *time* photocurrent response for the WS_2 monolayer area and WS_2/PEPI heterointerface area for 520 nm laser illumination with a power of 0.7 µW. The bias voltage V_{ds} equals 2 V and the gate voltage V_g equals 0 V.

3. I_{ds}-V_{ds} characteristics of the WS_2/PEPI heterostructure and WS_2 monolayer at low excitation power

Figure S3 displays I_{ds}-V_{ds} curves of the WS_2/PEPI heterostructure recorded for a 532 nm laser illumination with low excitation powers. The corresponding data for the WS_2 monolayer are displayed in Figure S4.

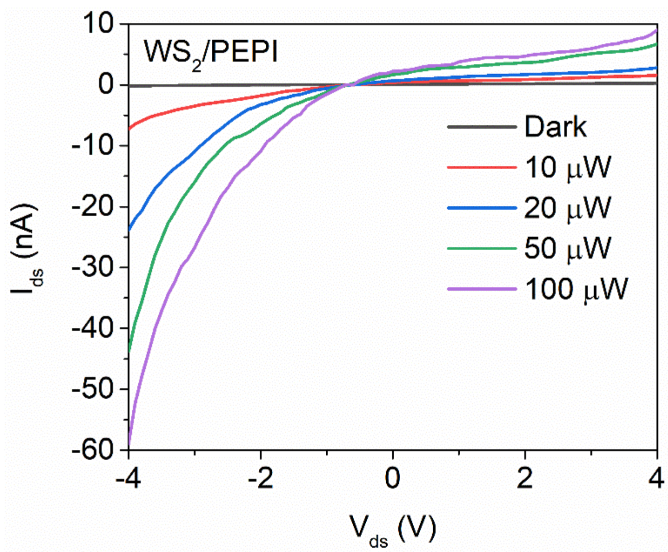

Figure S3. I_{ds}-V_{ds} characteristic for the WS_2/PEPI heterostructure in the dark and when illuminating the material with a 532 nm laser with laser power ranging from 10 µW to 100 µW.

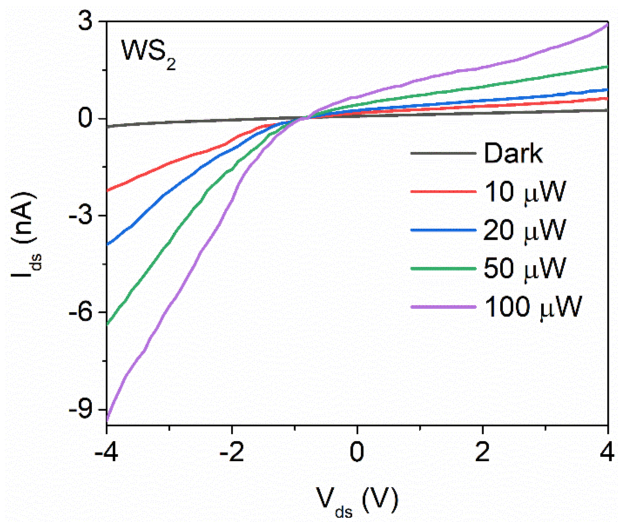

Figure S4. I_{ds}-V_{ds} characteristic for the WS_2 monolayer in the dark and when illuminating the material with a 532 nm laser with laser power ranging from 10 μW to 100 μW.

4. Current versus time photoresponse

The time dependent current photoresponse for a cyclical excitation for several laser intensities is illustrated in Figure S5 for the WS_2/PEPI heterostructure and in Figure S6 for the WS_2 monolayer. In both cases the drain to source bias voltage V_{ds} equals 2 V.

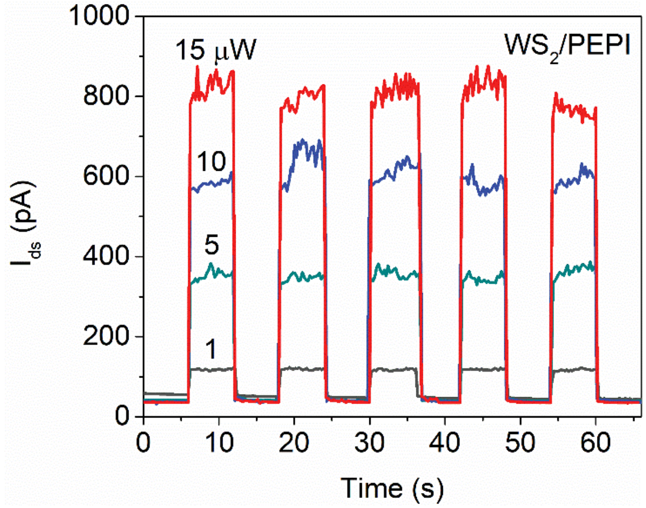

Figure S5. I_{ds}*-time* photocurrent response when the WS_2/PEPI heterostructure is periodically excited with a 532 nm laser with a power of 1 µW (black), 5 µW (cyan), 10 µW (blue), and 15 µW (red). The bias voltage V_{ds} is set to 2 V.

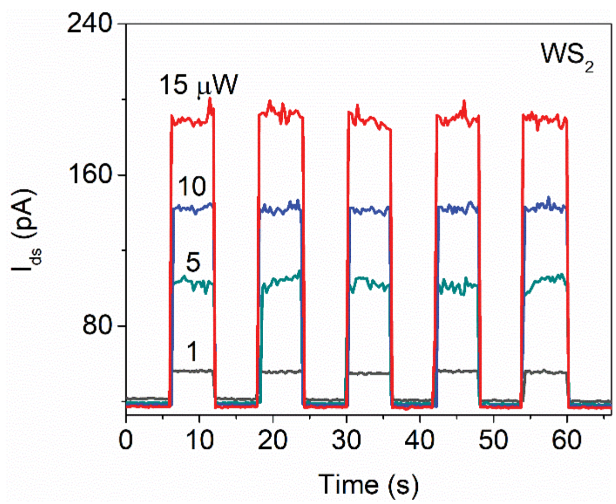

Figure S6. I_{ds}*-time* photocurrent response for the WS_2 monolayer for periodic excitation with a 532 nm laser with a power of 1 µW (black), 5 µW (cyan), 10 µW (blue), and 15 µW (red). The bias voltage V_{ds} is set to 2 V.